ACS APPLIED MATERIALS & INTERFACES

Article

Field-Effect Transistor Biosensor Platform Fused with Drosophila Odorant-Binding Proteins for Instant Ethanol Detection

Cheol-Min Lim, Jae Young Kwon, and Won-Ju Cho

ACS Appl. Mater. Interfaces, **Just Accepted Manuscript** • DOI: 10.1021/acsami.6b15539 • Publication Date (Web): 04 Apr 2017

ACS Publications

ACS Applied Materials & Interfaces is published by the American Chemical Society. 1155 Sixteenth Street N.W., Washington, DC 20036

Field-Effect Transistor Biosensor Platform Fused with Drosophila Odorant-Binding Proteins for Instant Ethanol Detection

Cheol-Min Lim,[†] *Jae Young Kwon,* [*,‡] *and Won-Ju Cho*[*,†]

[†]Department of Electronic Materials Engineering, Kwangwoon University, 20 Gwangwoon-ro, Nowon-gu, Seoul 01897, Republic of Korea

[‡]Department of Biological Sciences, Sungkyunkwan University, Seobu-ro, Jangan-gu, Suwon 440-746, Gyeonggi-do, Republic of Korea

KEYWORDS: odorant-binding protein, LUSH, olfactory biosensor, dual gate ISFET, ethanol

ABSTRACT

Odorant-binding proteins (OBPs) have attracted considerable attention as sensing substrates for the development of olfactory biosensors. The Drosophila LUSH protein is an OBP and is known to bind to various alcohols. Technology using the LUSH protein has great potential to provide crucial information through odorant detection. In this work, the LUSH protein was used as a sensing substrate to detect the ethanol concentration. Furthermore, we fused the LUSH protein with a silicon-on-insulator (SOI)-based ion-sensitive field-effect transistor (ISFET) to measure the electrical signals that arise from molecular interactions between LUSH and ethanol. A dual-gate sensing system for self-amplification of the signal resulting from molecular interaction between LUSH and ethanol was then applied to achieve much higher sensitivity than a conventional ISFET. In the results, we successfully detected ethanol with concentrations ranging between 0.001% and 1% by using the LUSH OBP-fused ISFET olfactory sensor. The OBP-fused olfactory SOI-based ISFET sensor can lead to the development of handheld sensors for various purposes such as detecting toxic chemicals, narcotics control, testing for food freshness, and non-invasive diagnoses.

INTRODUCTION

With the development of industrial technology, the use of harmful chemical gases has increased; this has led to a rise in leakage accidents related to dangerous gases. In order to prevent serious problems, the early detection of harmful agents is becoming increasingly important. However, some lethal or deadly toxic chemicals are nearly odorless and impossible to sense with the human nose in the early stages. Although such chemicals can be recognized after a long period of exposure, the body is most likely to receive significant damage before recognition. Even worse, some of these chemicals are absolutely odorless, which makes them highly dangerous to human. Therefore, there is a strong need for the development of a highly sensitive, fast, and accurate odorant sensor. In addition to public health concerns, highly sensitive, fast, and accurate odor detection can also be used in various situations such as narcotics control, diagnosing diseases from expiration, and testing the freshness of food.[1-3] Odorant-binding proteins (OBPs) are an activator for olfactory sensory neurons in Drosophila melanogaster and are a useful substrate class for detecting gas-borne analytes in sensory mimetic technology due to their high sensitivity and ease of production. By taking advantage of animals' olfactory systems, a highly sensitive odor sensor can be realized.[4-6]

OBP-based biosensors using a quartz crystal microbalance (QCM) or surface plasmon resonance (SPR) have previously been developed.[7-8] However, these biosensors have several drawbacks for practical applications: a high operation cost, difficulty with handling the equipment for the SPR sensor, and the slow detection time and lack of portability of the QCM sensor. To solve these problems and meet the need for sensory mimetic technology, the use of an ion-sensitive field-effect transistor (ISFET) has been proposed; this is a type of potentiometric sensor that measures ion concentrations in a solution and converts this into an electrical signal.[9-10] ISFETs can be used as a portable instrument for point-of-care testing (POCT) and offer desirable characteristics such as high sensitivity, low manufacturing cost, fast detection time, label-free detection, and portability.[11-12]

In this study, we developed an OBP-fused ISFET biosensor and demonstrated its feasibility for application as an olfactory sensor. To detect ethanol at various concentrations, a LUSH OBP, which is well-known to bind to various types of alcohols [13-15], was used as a sensing substrate. We also employed a dual-gate sensing system to enhance the signal produced by the molecular interaction between LUSH and ethanol. In the results, we successfully detected ethanol at concentration ranges of 0.001%–1%. The LUSH OBP-fused ISFET olfactory sensor can be a novel portable sensing tool to detect alcohols. This study demonstrated the potential application of OBP-fused ISFET olfactory sensors to the detection of various odorants besides ethanol.

EXPERIMENTAL SECTION

Preparation of the LUSH protein for sensing material: The LUSH protein was expressed from a plasmid containing LUSH cDNA with a sequence identical to a previously published cDNA clone.[16] The protein expression and purification process were custom-ordered from AB Frontier, Korea. Briefly, the LUSH cDNA was subcloned into a modified pET17b vector with a 6X His-thrombin cleavage site substituted for the T7 tag and overexpressed in Escherichia coli BL21 (DE3). The His-tagged LUSH protein was purified under denaturing conditions using Ni-NTA affinity columns, and the purity of the ~14 kDa LUSH protein was assessed for each eluted fraction on a 15% SDS-PAGE gel. The cleanest fractions were pooled and concentrated to a final concentration of 1 mg/ml in a storage buffer (8 M Urea, 50 mM NaH_2PO_4, 300 mM NaCl, 500 mM imidazole (pH 8), 10% glycerol). Aliquots of the final protein solution were stored at –80 °C until further use.

ISFET fabrication procedure: ISFETs were designed from standard metal–oxide–semiconductor field-effect transistors (MOSFETs) and are composed of two parts: a detector to detect information from the cell, DNA, antigen-antibody, and enzyme; and a transducer that converts this to changes in potential for recognition.[17] As shown in Figure 1(a), we separated the sensitive membrane (sensing part) from the FET (transducer part) to obtain several advantages: a disposable sensitive membrane, reusable FETs, minimized ion damage to the FET due to undesirable ions in the sensitive membrane, and insensitivity to temperature and light.[18]

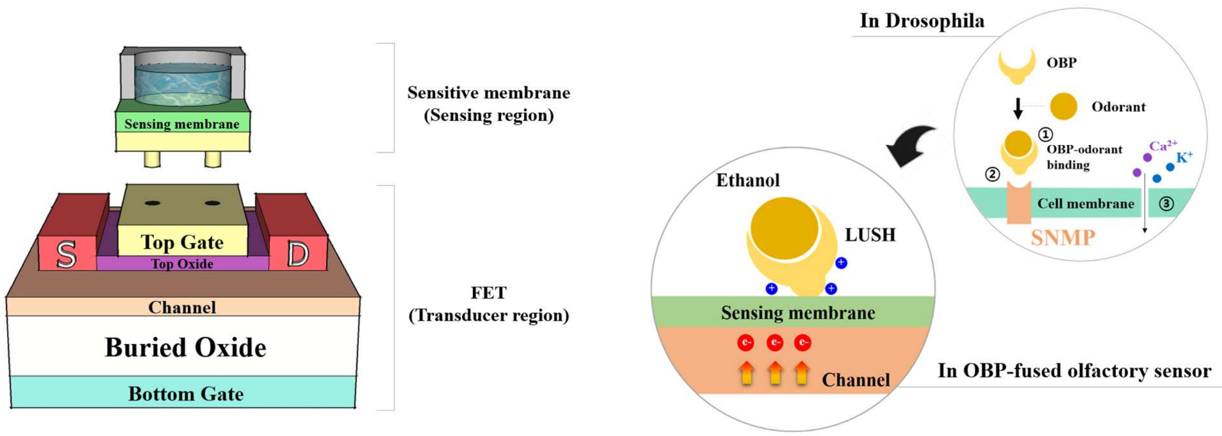

(a) (b)

Figure 1. (a) Schematic representation of ISFET with a separated sensitive membrane. (b) Odorant sensing mechanism of Drosophila OBP-fused olfactory sensor.

Fabrication of SOI-based FET (transducer part): To fabricate the FET for the transducer part, p-type (100) silicon-on-insulator (SOI) wafers with a 100-nm-thick top silicon layer and 750-nm-thick buried oxide (BOX) layer was used. The resistivity and doping level of top silicon layer were 10 Ω·cm and 1×10^{15} cm^{-3}, respectively. At first, the top silicon of 100-nm-thick thickness was etched to a thickness of 10 nm using 2.38% tetramethylammonium hydroxide (TMAH) solution. After the active region was formed by photolithography and the reactive ion etching (RIE) process, a 100-nm-thick phosphorus-doped polycrystalline silicon (poly-Si) layer was deposited at the source/drain (S/D) regions by low-pressure chemical vapor deposition (LPCVD). Subsequently, a gate dielectric layer with a thickness of 10 nm was grown by thermal oxidation. To improve the conductivity of the doped poly-Si S/D, rapid thermal annealing (RTA) was performed at 850 ° C for 30 s in N_2/O_2 ambient gas. Finally, an Al gate electrode was formed with a thickness of 150 nm with an e-beam evaporator followed by forming gas annealing at 450 °C for 30 min in a 2% H_2/N_2 ambient to reduce the dangling bonds and defects at the interface region. The channel length and width of the fabricated device were 10 and 20 μm, respectively. In addition, the bottom silicon substrate of the SOI MOSFET worked as the bottom gate (BG) electrode.

Fabrication of separated sensitive membrane (sensing part): To fabricate a separated sensing electrode, a p-type Si (100) wafer with a 300-nm-thick thermal SiO_2 layer was used as the substrate. After a 100-nm-thick Al electrode was deposited to transmit the changes in surface potential on the sensing membrane to the top gate (TG) of the FET, a 50-nm-thick tin dioxide (SnO_2) sensing membrane was deposited by RF magnetron sputtering. The RF power, chamber pressure, and Ar gas flow rate were maintained at 50 W, 3 mTorr, and 20 sccm, respectively. Finally, the polydimethylsiloxane (PDMS) reservoir with an internal diameter of 0.8 cm was attached to the sensing membrane with silicone glue. The separated sensing electrode was connected to the TG electrode of the SOI MOSFET. Figure 1(a) shows a schematic representation of the fabricated ISFET.

Operational mechanism of SOI-based ISFET: The fabricated ISFET has two sensing mode operations: single gate (SG) and dual gate (DG). The sensing characteristics of the SG mode were measured by biasing the top reference electrode with a grounded BG. In contrast, the sensing characteristics of the DG mode were investigated by scanning the voltage on the BG with a grounded top reference electrode. The description of a SG and DG operation mode is shown in Figure S1. Generally, conventional ISFETs are driven by a SG sensing mode, and their maximum achievable sensitivity (i.e., the Nernstian sensitivity) is limited to 59 mV/pH at 25 °C.[19] This is because the sensitivity ΔV^{T}_{th} is determined only by the change in surface potential $\Delta\psi_0$ of the sensing membrane: $\Delta V^{T}_{th} = -\Delta\psi_0$. In contrast, the ISFET constructed in this work is driven by a DG sensing mode, and its sensitivity ΔV^{B}_{th} depends on not only $\Delta\psi_0$ but also the ratio between the top and bottom gate capacitances:

$$\Delta V^{B}_{th} = -\frac{C_{top}}{C_{bottom}}\Delta\psi_0 = \frac{C_{top}}{C_{bottom}}\Delta V^{T}_{th} \quad (1)$$

where C_{top} and C_{bottom} are the top and bottom gate capacitances per unit area, respectively.[20] Therefore, the limit of Nernstian sensitivity can be overcome under the condition of $C_{top} >> C_{bottom}$.[21-25]

Odorant sensing mechanism: Figure 1(b) describes the odorant sensing mechanism of Drosophila and an OBP-fused olfactory sensor. Drosophila perceives an odorant when sensory neurons are activated by the OBP-odorant complex.[14, 26] The overall odorant perception mechanism is as follows: (1) when an OBP binds to an odorant, the OBP transports its odorant to a sensory neuron membrane protein (SNMP)[27]; (2) the SNMP is activated by the OBP-odorant complex[16]; and (3) the activated SNMP relieves the SNMP-mediated inhibition, which opens ion channels and allows cations to enter the neurons.[28] This mechanism was applied to the OBP-fused olfactory sensor. To detect the ethanol, we used the LUSH protein as an OBP. When LUSH responds to ethanol, the change in the surface charge of LUSH cause the channel resistance in the FET sensor to vary.[3]

Measurements of ISFETs: To investigate the pH sensing behavior and ethanol detection, the drain current versus gate voltage (I_D–V_G) curves of ISFET were measured by using an Agilent 4156B precision semiconductor parameter analyzer. RE-5B Ag / AgCl reference electrode purchased from EChem Market was used, and all measurements were conducted in a dark box to avoid interference from light and external noise. We purchased the pH buffer solutions (pH 3, 4, 6, 7, 9, 10) from Samchun Pure Chemical in Korea.

Measurement protocol for detecting LUSH–ethanol interaction: For detection of ethanol, we monitored the change of electrical characteristics by measuring the electrical characteristics (I_D-V_G curve) before and after ethanol injection after LUSH injection. The principle of immobilization that the LUSH receptors stick to the sensing membrane is simply that the LUSH receptors sink to the bottom of the solution and then physisorb to the sensing membrane. To confirm only the effect of the reaction between LUSH and ethanol, the experiments were carried out under all the same conditions (including device) and only the concentration of ethanol was changed. In order to demonstrate the molecular interactions between LUSH and ethanol (EtOH), we carried out three different experiments as shown in Figure 2: (a) LUSH–EtOH interaction (sensing test), (b) LUSH–DI water interaction (control test #1), and (c) PBS–EtOH interaction (control test #2). The measurement protocol for detecting the LUSH–EtOH interaction is as follows: (1) inject 100 µl of 750 µg/ml LUSH protein solution into the chamber, (2) measure the initial drain current I_D while forcing a constant voltage (V_{TG}: 1 V, V_D: 50 mV, V_{BG} and V_S: 0 V) until I_D is stabilized, (3) inject 30 µl of ethanol at a concentration of 0.001% and measure I_D 20 s after an equilibrium state of interaction is reached, and (4) repeat the same procedure by injecting 0.01, 0.1, 1% v/v ethanol diluted in water from low concentrations. For the LUSH–DI water interaction, DI water was used as the control analyte solution instead of ethanol. In the case of the PBS–EtOH interaction a 0.01× PBS solution was used as the control sensing substrate instead of the LUSH protein. In the control experiments, to minimize the influence on ethanol and LUSH reaction, DI water and PBS were selected as controls. Control measurements were conducted under the same conditions as the main sensing experiments.

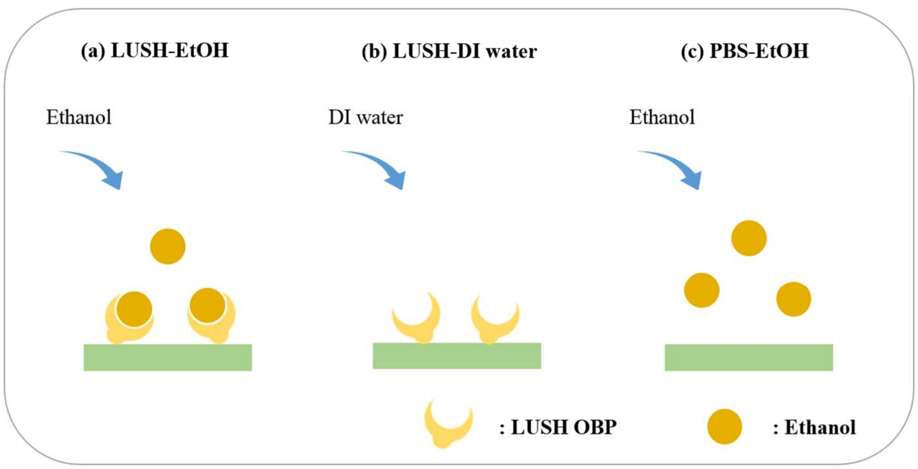

Figure 2. Schematic illustrations of (a) LUSH–EtOH, (b) LUSH–DI water, and (c) PBS–EtOH interactions.

RESULTS AND DISCUSSION

The electrical characteristics of SOI MOSFET were measured to evaluate its functionality as a transducer of ISFET. Figure 3 shows the transfer curve (I_D–V_G) of SOI MOSFET for TG or BG sweep methods. TG sweep mode were measured by biasing the top gate with a grounded BG. In contrast, BG sweep mode were measured by biasing the bottom gate voltage with a grounded top gate. Figures S2(a) and (b) exhibit the schematic representation of FET in TG and BG sweep method, respectively. Table 1 summarizes the electrical parameters extracted from the two sweep modes. In the case of the TG sweep mode, Figure 3(a) shows that the TG MOSFET performed well with a low threshold voltage V_{th} of –0.34 V, a good subthreshold swing SS of 64.58 mV/dec, and high on/off current ratio of 4.50×10^9. Meanwhile, Figure 3(b) shows that the BG MOSFET demonstrated good characteristics, including V_{th} of -2.48 V, SS of 485.31 mV/dec, and an on/off current ratio of 7.01×10^{10} despite the BG oxide (750 nm) being much thicker than the TG oxide (10 nm). This result implies that the SOI MOSFET has sufficient characteristics to function as an ISFET transducer.

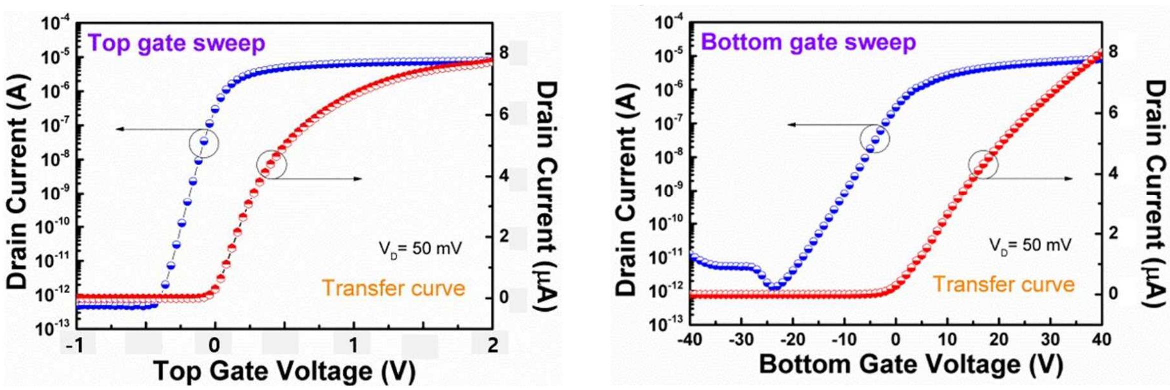

(a) (b)

Figure 3. Transfer curves of SOI MOSFET swept by (a) TG and (b) BG.

Table 1. Electrical characteristics of SOI MOSFET according to the gate sweep methods.

Sweep mode	V_{th} [V]	*SS* [mV/dec]	Maximum on/off current ratio
TG	–0.34	64.58	4.50×10^9
BG	–2.48	485.31	7.01×10^8

To observe then amplifying action with an SOI-based ISFET in DG sensing mode, we evaluated the sensing properties of ISFET in SG and DG sensing modes. Figures 4(a) and (b) show the I_D–V_G curves of the ISFET in the SG and DG sensing modes at various pH levels.

When the pH solution was changed from pH 3 to pH 10, the reference voltage V_R, which is the corresponding gate voltage V_G to the reference current I_R, consistently shifted to the positive V_G direction. Figure 4(a) shows that the ISFET in SG sensing mode exhibited a sensitivity of 58.69 mV/pH close to the Nernstian limit (59 mV/pH). Meanwhile, Figure 4(b) shows that the sensitivity of the DG mode markedly increased to 3723.12 mV/pH, which is 63-fold larger than the Nernstian limit. Here, note that the enhanced sensitivity of the SOI-based ISFET in DG sensing mode does not mean a simple improvement of the signal-to-noise ratio. In our previous work, we demonstrated that the relative reliability and stability of ISFET in DG sensing mode can be improved to a greater degree than those of ISFET in SG sensing mode.[29-30]

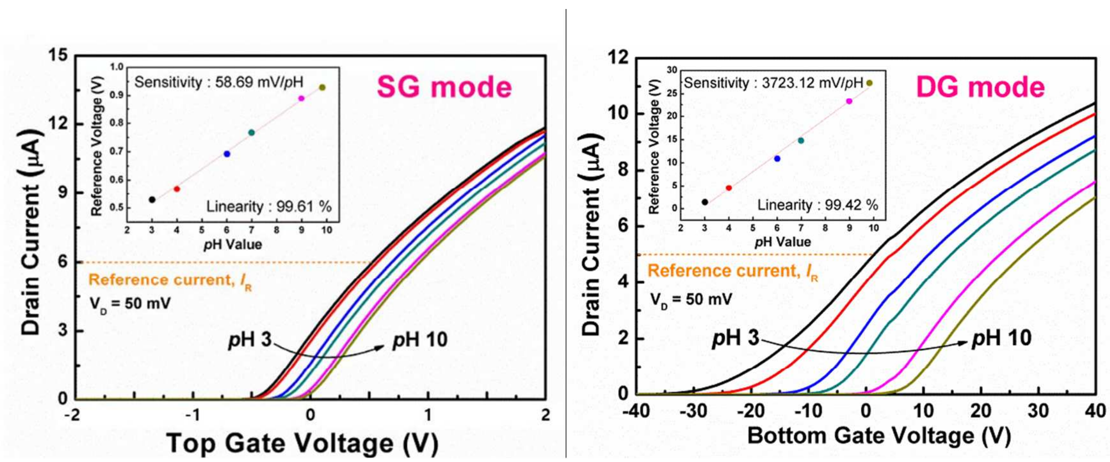

(a) (b)

Figure 4. I_D–V_G curves of SOI-based ISFET under (a) SG sensing and (b) DG sensing modes at various pH levels. The drain bias was set to 50 mV. In the inset, V_R at each pH level was defined as the corresponding gate voltage to a drain current (reference current I_R) of 6 μA for the ISFET in SG sensing mode and 5 μA for the ISEFT in DG sensing mode.

Figure 5(a) represents the variation in the drain current ΔI_D depending on the ethanol concentration during the LUSH–EtOH, LUSH–DI water, and PBS–EtOH interactions. I_D in the LUSH–EtOH interaction increased in a dose-dependent manner with an increasing ethanol concentration, whereas I_D in the LUSH–DI water interaction showed little change. In order to evaluate whether the ethanol injection itself could cause a change in I_D, we examined changes in I_D with a PBS–EtOH interaction. Although a slight change in I_D was observed, the magnitude of ΔI_D was much smaller than that of the LUSH–EtOH interaction. This indicates that the electrical signals generated from the LUSH–EtOH interaction are most likely due to the molecular interactions rather than being a side effect of the ethanol injection. To confirm the cause of the electrical signal, the zeta potential of LUSH protein was measured by Electrophoretic Light Scattering Spectrophotometer (ELS-8000, Otsuka Electronics). The results showed that the zeta potential of the LUSH protein decreased with an increasing ethanol concentration (Figure S3). This means that the surface of the LUSH protein becomes negatively charged as LUSH binds ethanol.[3, 31] The negative surface charge of LUSH attracts the positive ions in the solution, and these congregated positive ions contribute to make the surface potential ψ_0 of the sensing membrane more positive.[32-33] Consequently, the additional positive surface potential ψ_0 yields a low channel resistance for the transistor, which increases I_D.[34] We repeated the same experiment three times to demonstrate the reproducibility. Figure 5(b) shows the results of the reproducibility tests for the LUSH–EtOH, LUSH–DI water, and PBS–EtOH interactions. To facilitate data comparison, we extracted the final points of each time interval for each ethanol concentration from the data. In all of the experiments, the LUSH–EtOH, LUSH–DI water, and PBS–EtOH interactions showed good reproducibility. In order to evaluate the interaction intensities depending on the LUSH concentration, 1 mg/ml LUSH protein stock solution was diluted with 0.01× PBS solution to 250, 500, and 750 µg/ml. Figure 5(c) shows the variation in the sensing margin current depending on the LUSH concentration. The sensing margin current was defined as the difference between the variations in I_D for the LUSH–EtOH and PBS–EtOH interactions. Experiments were performed three times to evaluate the reproducibility, and the same procedure as that of the previous experiment was repeated. The results showed that the sensing margin current increased with the concentration of the LUSH protein. This implies that the magnitude of the electrical signal to detect the ethanol concentration can be controlled by adjusting the LUSH concentration. The results of Figure 5 clearly show that the molecular interactions between the LUSH protein and ethanol were detected.

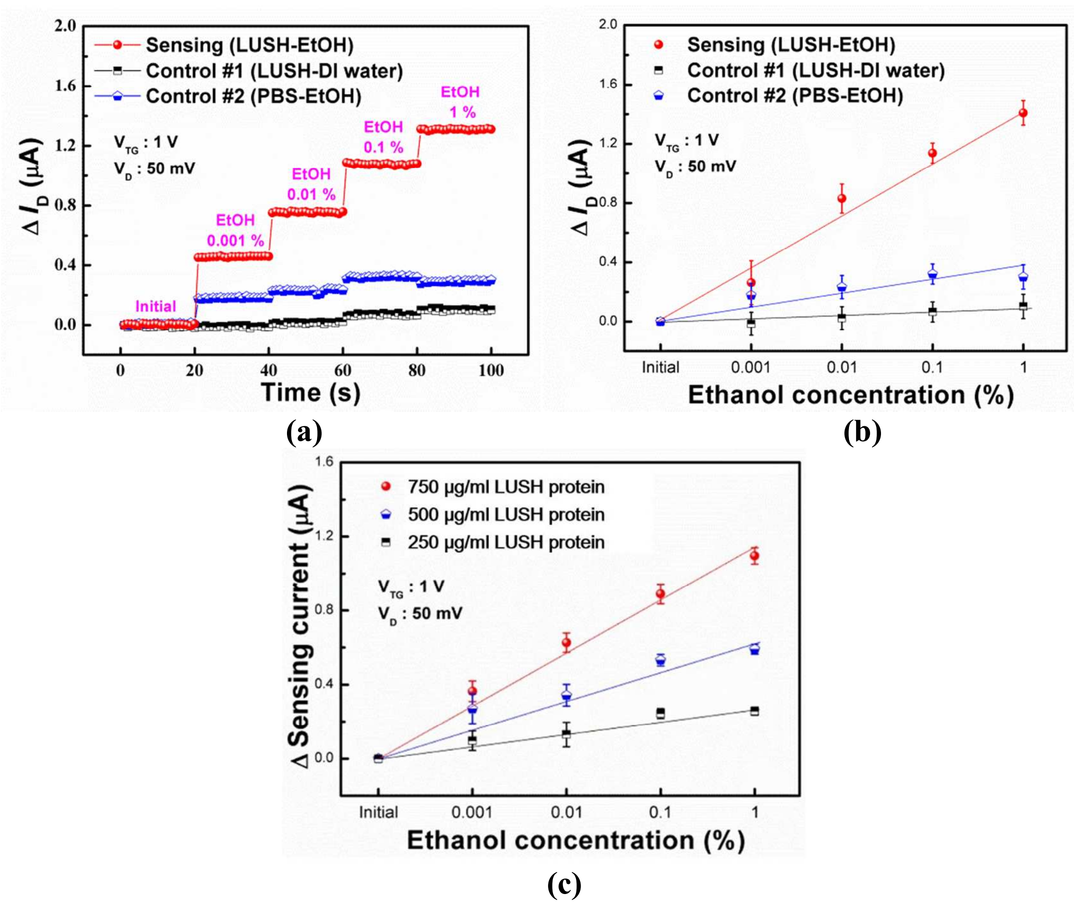

Figure 5. (a) Variations in the drain current ΔI_D according to the ethanol concentration with LUSH–EtOH, LUSH–DI water, and PBS–EtOH interactions. (b) Reproducibility test results for the LUSH–EtOH, LUSH–DI water, and PBS–EtOH interactions. (c) Variations in the sensing margin current depending on the LUSH concentration.

In order to detect the ethanol concentration with greater sensitivity, we exploited the SOI-based ISFET in DG sensing mode (LUSH-fused olfactory sensor). Figures 6(a) and (b) show the I_D–V_G curves for different ethanol concentrations during LUSH–EtOH and PBS–EtOH interactions, respectively. As shown in Figure 6(a), V_{th} in the LUSH–EtOH interaction shifted to the negative direction as the ethanol concentration increased. On the other hand, Figure 6(b) shows no shift in V_{th} for the PBS–EtOH interaction. The negative shift in V_{th} with the LUSH–EtOH interaction was due to a change in the channel resistance, as noted earlier. These results indicate that our LUSH OBP-fused olfactory sensor in DG sensing mode has a high sensitivity and outstanding specificity for detecting ethanol in a detection range from 0.001% to 1%. Figure 6(c) shows the variation in V_R (ΔV_R) corresponding to each ethanol concentration with the LUSH–EtOH interaction when using the SOI-based ISFET in SG and DG sensing modes (I_D-V_G curves of ISEFT under SG mode according to ethanol concentration in LUSH-EtOH interaction are shown in Figure S4). The sensitivity of ethanol can be extracted by calculating the average ΔV_R per decade of ethanol concentration. In the results, the ethanol sensitivities of SOI-based ISFETs in SG and DG sensing modes were 1.99 and 129.45 mV/dec, respectively. Note that the DG sensing mode showed a 65-fold enhancement in signal sensing compared with the SG sensing mode. This means that the SOI-based ISFET in DG sensing mode can enhance not only the sensing signal but also the detection limit of the target molecule concentration.

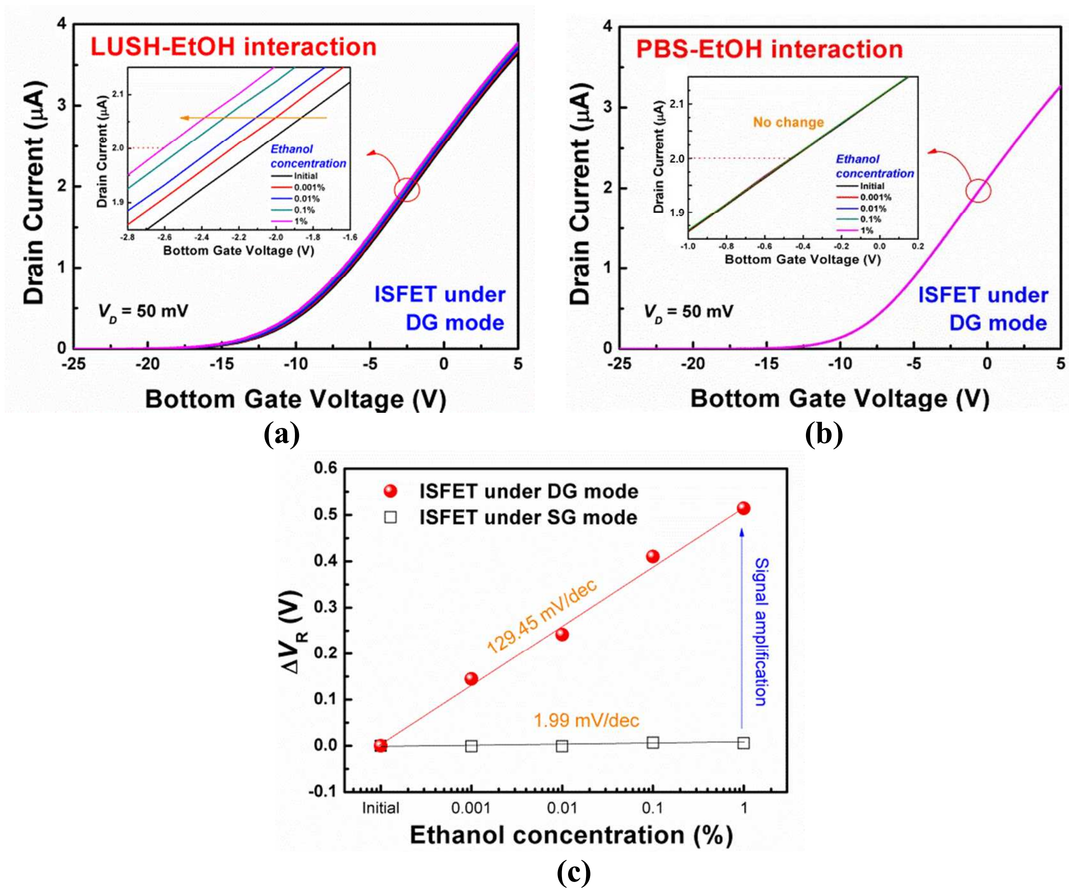

Figure 6. I_D–V_G curves of SOI-based ISFET in DG sensing mode according to different ethanol concentrations with the (a) LUSH–EtOH and (b) PBS–EtOH interactions. The drain bias was set to 50 mV. (c) Variations in V_R (ΔV_R) corresponding to each ethanol concentration. Here, V_R was defined as the corresponding gate voltage to the drain current of 2 μA for the ISFET in DG mode and 6 μA for the ISFET in SG mode.

CONCLUSION

We developed an OBP-fused ISFET olfactory sensor that detects odorants. To demonstrate its feasibility as an olfactory sensor, we used the Drosophila LUSH protein as a sensing substrate and detected ethanol at a concentration range of 0.001%–1% by using a LUSH OBP-fused transistor olfactory sensor. By adapting the DG sensing mode of an SOI-based ISFET, we successfully detected the ethanol concentration with a high sensitivity of 129.45 mV/dec. The proposed OBP-fused ISFET olfactory sensor offers a new avenue for the development of portable sensors that can be applied to various situations, such as non-invasive diagnosis of diseases, the detection of toxic chemicals, narcotics control, and testing food for freshness.

ASSOCIATED CONTENT

AUTHOR INFORMATION

Corresponding Authors

E-mail address: chowj@kw.ac.kr (W.-J. Cho)

E-mail address: jaeyoung.kwon@gmail.com (J. Y. Kwon)

Notes

The authors declare no competing financial interest.

Author Contributions

The manuscript was written through the contributions of all authors. All authors have given approval to the final version of the manuscript.

ACKNOWLEDGMENT

This research was financially supported by Basic Science Research Program through the National Research Foundation of Korea (NRF) funded by the Science and Technology (No. 2016R1A2B4008754).

Supporting Information. This material is available free of charge via the Internet at http://pubs.acs.org.

The description of SG operation mode and DG operation mode, schematic representation of FET in top gate sweep method and back gate sweep method, zeta potential distributions of the LUSH protein according to ethanol concentration, I_D-V_G curves of the ISFET under SG mode according to different ethanol concentrations in LUSH-EtOH interaction.

REFERENCES

1. Nowotny, T.; de Bruyne, M.; Berna, A. Z.; Warr, C. G.; Trowell, S. C. Drosophila Olfactory Receptors as Classifiers for Volatiles from Disparate Real World Applications. *Bioinspiration Biomimetics* **2014,** *9*, 046007.
2. Sankaran, S.; Panigrahi, S.; Mallik, S. Odorant Binding Protein based Biomimetic Sensors for Detection of Alcohols Associated with Salmonella Contamination in Packaged Beef. *Biosens. Bioelectron.* **2011,** *26*, 3103-3109.
3. Kim, T. H.; Lee, S. H.; Lee, J.; Song, H. S.; Oh, E. H.; Park, T. H.; Hong, S. Single carbon atomic resolution Detection of Odorant Molecules using a Human Olfactory Receptor based Bioelectronic Nose. *Adv. Mater. Interfaces* **2009,** *21*, 91-94.
4. Lu, Y.; Yao, Y.; Zhang, Q.; Zhang, D.; Zhuang, S.; Li, H.; Liu, Q. Olfactory Biosensor for Insect Semiochemicals Analysis by Impedance Sensing of Odorant-binding Proteins on Interdigitated Electrodes. *Biosens. Bioelectron.* **2015,** *67*, 662-669.
5. Mulla, M. Y.; Tuccori, E.; Magliulo, M.; Lattanzi, G.; Palazzo, G.; Persaud, K.; Torsi, L. Capacitance-modulated Transistor Detects Odorant Binding Protein Chiral Interactions. *Nat. Commun.* **2015,** *6,* 6010.
6. Ko, H. J.; Park, T. H. Enhancement of Odorant Detection Sensitivity by the Expression of Odorant-binding Protein. *Biosens. Bioelectron.* **2008,** *23*, 1017-1023.
7. Lee, S. H.; Ko, H. J.; Park, T. H. Real-time Monitoring of Odorant-induced Cellular Reactions using Surface Plasmon Resonance. *Biosens. Bioelectron.* **2009,** *25*, 55-60.
8. Kimura, M.; Sakai, R.; Sato, S.; Fukawa, T.; Ikehara, T.; Maeda, R.; Mihara, T. Sensing of Vaporous Organic Compounds by TiO2 Porous Films Covered with Polythiophene Layers. *Adv. Funct. Mater.* **2012,** *22*, 469-476.
9. Bergveld, P. Thirty years of ISFETOLOGY: What Happened in the Past 30 Years and What May Happen in the Next 30 Years. *Sens. Actuators, B* **2003,** *88*, 1-20.
10. Schöning, M. J.; Poghossian, A. Bio FEDs (Field Effect Devices): State-of-the-Art and New Directions. *Electroanalysis* **2006,** *18*, 1893-1900.

11. Makowski, M. S.; Ivanisevic, A. Molecular Analysis of Blood with Micro□/Nanoscale Field□Effect□Transistor Biosensors. *Small* **2011,** *7*, 1863-1875.
12. Leleux, P.; Rivnay, J.; Lonjaret, T.; Badier, J. M.; Bénar, C.; Hervé, T.; Chauvel, P.; Malliaras, G. G. Organic Electrochemical Transistors for Clinical Applications. *Adv. Healthcare Mater.* **2015,** *4*, 142-147.
13. Kim, M.-S.; Repp, A.; Smith, D. P. LUSH Odorant-binding Protein Mediates Chemosensory Responses to Alcohols in Drosophila Melanogaster. *Genetics* **1998,** *150*, 711-721.
14. Stowers, L.; Logan, D. W. LUSH Shapes Up for a Starring Role in Olfaction. *Cell* **2008,** *133*, 1137-1139.
15. Ader, L.; Jones, D. N.; Lin, H. Alcohol Binding to the Odorant Binding Protein LUSH: Multiple Factors Affecting Binding Affinities. *Biochemistry* **2010,** *49*, 6136-6142.
16. Kruse, S. W.; Zhao, R.; Smith, D. P.; Jones, D. N. Structure of a Specific Alcohol-binding Site Defined by the Odorant Binding Protein LUSH from Drosophila Melanogaster. *Nat. Struct. Mol. Biol.* **2003,** *10*, 694-700.
17. Batista, P.; Mulato, M. ZnO Extended-gate Field-effect Transistors as pH Sensors. *Appl. Phys. Lett.* **2005,** *87*, 143508-143900.
18. Chen, J.-C.; Chou, J.-C.; Sun, T.-P.; Hsiung, S.-K. Portable Urea Biosensor based on the Extended-gate Field Effect Transistor. *Sens. Actuators, B* **2003,** *91*, 180-186.
19. Knopfmacher, O.; Tarasov, A.; Fu, W.; Wipf, M.; Niesen, B.; Calame, M.; Schonenberger, C. Nernst Limit in Dual-gated Si-nanowire FET Sensors. *Nano Lett.* **2010,** *10*, 2268-2274.
20. Spijkman, M. J.; Brondijk, J. J.; Geuns, T. C.; Smits, E. C.; Cramer, T.; Zerbetto, F.; Stoliar, P.; Biscarini, F.; Blom, P. W.; de Leeuw, D. M. Dual-gate Organic Field-effect Transistors as Potentiometric Sensors in Aqueous Solution. *Adv. Funct. Mater.* **2010,** *20*, 898-905.
21. Spijkman, M.; Smits, E.; Cillessen, J.; Biscarini, F.; Blom, P.; de Leeuw, D. Beyond the Nernst-limit with Dual-gate ZnO Ion-sensitive Field-effect Transistors. *Appl. Phys. Lett.* **2011,** *98*, 043502.
22. Spijkman, M. J.; Myny, K.; Smits, E. C.; Heremans, P.; Blom, P. W.; de Leeuw, D. M. Dual□Gate Thin□Film Transistors, Integrated Circuits and Sensors. *Adv. Mater. Interfaces* **2011,** *23*, 3231-3242.
23. Lim, H.-K.; Fossum, J. G. Threshold Voltage of Thin-film Silicon-on-insulator (SOI) MOSFET's. *IEEE Trans. Electron Devices* **1983,** *30*, 1244-1251.
24. Jang, H.-J.; Bae, T.-E.; Cho, W.-J. Improved Sensing Performance of Polycrystalline-silicon based Dual-gate Ion-sensitive Field-effect Transistors using High-k Stacking Engineered Sensing Membrane. *Appl. Phys. Lett.* **2012,** *100*, 253703.
25. Park, J.-K.; Jang, H.-J.; Park, J.-T.; Cho, W.-J. SOI dual-gate ISFET with Variable Oxide Capacitance and Channel Thickness. *Solid-State Electron.* **2014,** *97*, 2-7.
26. Firestein, S. How the Olfactory System Makes Sense of Scents. *Nature* **2001,** *413*, 211-218.
27. Chen, C.; Abe, K.; Kumomi, H.; Kanicki, J. a□InGaZnO Thin-film Transistors for AMOLEDs: Electrical Stability and Pixel-circuit Simulation. *J. Soc. Inf. Disp.* **2009,** *17*, 525-534.

28. Lim, J. H.; Park, J.; Oh, E. H.; Ko, H. J.; Hong, S.; Park, T. H. Nanovesicle□Based Bioelectronic Nose for the Diagnosis of Lung Cancer from Human Blood. *Adv. Healthcare Mater.* **2014,** *3*, 360-366.
29. Bae, T.-E.; Cho, W.-J. Enhanced Sensing Properties of Fully Depleted Silicon-on-Insulator-Based Extended-Gate Field-Effect Transistor with Dual-Gate Operation. *Appl. Phys. Express* **2013,** *6*, 127001.
30. Lee, I.-K.; Lee, K. H.; Lee, S.; Cho, W.-J. Microwave Annealing Effect for Highly Reliable Biosensor: Dual-Gate Ion-Sensitive Field-Effect Transistor Using Amorphous InGaZnO Thin-Film Transistor. *ACS Appl. Mater. Interfaces* **2014,** *6*, 22680-22686.
31. Chen, R. J.; Choi, H. C.; Bangsaruntip, S.; Yenilmez, E.; Tang, X.; Wang, Q.; Chang, Y.-L.; Dai, H. An Investigation of the Mechanisms of Electronic Sensing of Protein Adsorption on Carbon Nanotube Devices. *J. Am. Chem. Soc.* **2004,** *126*, 1563-1568.
32. Gonçalves, D.; Prazeres, D.; Chu, V.; Conde, J. Detection of DNA and Proteins using Amorphous Silicon Ion-sensitive Thin-film Field Effect Transistors. *Biosens. Bioelectron.* **2008,** *24*, 545-551.
33. Sakata, T.; Ihara, M.; Makino, I.; Miyahara, Y.; Ueda, H. Open Sandwich-based Immuno-transistor for Label-free and Noncompetitive Detection of Low Molecular Weight Antigen. *Anal. Chem.* **2009,** *81*, 7532-7537.
34. Jang, H.-J.; Ahn, J.; Kim, M.-G.; Shin, Y.-B.; Jeun, M.; Cho, W.-J.; Lee, K. H. Electrical Signaling of Enzyme-linked Immunosorbent Assays with an Ion-sensitive Field-effect Transistor. *Biosens. Bioelectron.* **2015,** *64*, 318-323.

Table of Contents